


## RESEARCH ARTICLE

# Transcranial Magnetic Stimulation Exerts “Rejuvenation” Effects on Corticostriatal Synapses after Partial Dopamine Depletion

Giuseppina Natale, MSc,<sup>1,2</sup> Annabella Pignataro, PhD,<sup>3,4</sup> Gioia Marino, MSc,<sup>1,2</sup> Federica Campanelli, PhD,<sup>2</sup> Valeria Calabrese, MSc,<sup>1,5</sup> Antonella Cardinale, PhD,<sup>2,5</sup> Silvia Pelucchi, PhD,<sup>6</sup> Elena Marcello, PhD,<sup>6</sup> Fabrizio Gardoni, PhD,<sup>6</sup> Maria Teresa Viscomi, PhD,<sup>7</sup> Barbara Picconi, PhD,<sup>5,10</sup> Martine Ammassari-Teule, PhD,<sup>4,8</sup> Paolo Calabresi, MD,<sup>2,9</sup> and Veronica Ghiglieri, PhD<sup>10,11\*</sup> 

<sup>1</sup>Department of Medicine, University of Perugia, Perugia, Italy

<sup>2</sup>Dipartimento di Neuroscienze, Facoltà di Medicina e Chirurgia, Università Cattolica del Sacro Cuore, Rome, Italy

<sup>3</sup>Institute of Translational Pharmacology (IFT) National Research Council, Rome, Italy

<sup>4</sup>Laboratory of Psychobiology, IRCCS Fondazione Santa Lucia c/o CERC, Rome, Italy

<sup>5</sup>IRCCS San Raffaele Pisana, Rome, Italy

<sup>6</sup>Department of Pharmacological and Biomolecular Sciences, University of Milano, Milan, Italy

<sup>7</sup>Department of Life Sciences and Public Health Section Histology and Embryology, Università Cattolica del Sacro Cuore, Rome, Italy

<sup>8</sup>Institute of Biochemistry and Cell Biology (IBBC), National Research Council, Rome, Italy

<sup>9</sup>Neurologia, Fondazione Policlinico Universitario Agostino Gemelli IRCCS, Rome, Italy

<sup>10</sup>San Raffaele University, Rome, Italy

<sup>11</sup>Laboratory of Neurophysiology, IRCCS Fondazione Santa Lucia c/o CERC, Rome, Italy

**ABSTRACT: Background:** In experimental models of Parkinson's disease (PD), different degrees of degeneration to the nigrostriatal pathway produce distinct profiles of synaptic alterations that depend on progressive changes in N-methyl-D-aspartate receptors (NMDAR)-mediated functions. Repetitive transcranial magnetic stimulation (rTMS) induces modifications in glutamatergic and dopaminergic systems, suggesting that it may have an impact on glutamatergic synapses modulated by dopamine neurotransmission. However, no studies have so far explored the mechanisms of rTMS effects at early stages of PD.

**Objectives:** We tested the hypothesis that in vivo application of rTMS with intermittent theta-burst stimulation (iTBS) pattern alleviates corticostriatal dysfunctions by modulating NMDAR-dependent plasticity in a rat model of early parkinsonism.

**Methods:** Dorsolateral striatal spiny projection neurons (SPNs) activity was studied through ex vivo whole-cell patch-clamp recordings in corticostriatal slices obtained from 6-hydroxydopamine-lesioned rats, subjected to a single session (acute) of iTBS and tested for forelimb akinesia with the stepping test. Immunohistochemical

analyses were performed to analyze morphological correlates of plasticity in SPNs.

**Results:** Acute iTBS ameliorated limb akinesia and rescued corticostriatal long-term potentiation (LTP) in SPNs of partially lesioned rats. This effect was abolished by applying a selective inhibitor of GluN2B-subunit-containing NMDAR, suggesting that iTBS treatment could be associated with an enhanced activation of specific NMDAR subunits, which are major regulators of structural plasticity during synapse development. Morphological analyses of SPNs revealed that iTBS treatment reverted dendritic spine loss inducing a prevalence of thin-elongated spines in the biocytin-filled SPNs.

**Conclusions:** Taken together, our data identify that an acute iTBS treatment produces a series of plastic changes underlying striatal compensatory adaptation in the parkinsonian basal ganglia circuit. © 2021 The Authors. *Movement Disorders* published by Wiley Periodicals LLC on behalf of International Parkinson and Movement Disorder Society

**Key Words:** striatum; dendritic spines; GluN2B; partial dopamine denervation; noninvasive brain stimulation

This is an open access article under the terms of the Creative Commons Attribution-NonCommercial License, which permits use, distribution and reproduction in any medium, provided the original work is properly cited and is not used for commercial purposes.

\*Correspondence to: Prof. Veronica Ghiglieri, San Raffaele University, Via di Val Cannuta, 247 00166 Rome, Italy; E-mail: veronica.ghiglieri@uniroma5.it

Giuseppina Natale and Annabella Pignataro contributed equally.

**Relevant conflicts of interest/financial disclosures:**

**Funding agencies:** This work was supported by grants from the Fresco Parkinson Institute to New York University School of Medicine and The Marlene and Paolo Fresco Institute for Parkinson's and Movement Disorders, which were made possible with support from Marlene and Paolo Fresco (V.G., P.C., and A.C.) and by the Italian Ministry of Health, Ricerca Corrente (B.P. and P.C.).

**Received:** 31 January 2021; **Revised:** 8 May 2021; **Accepted:** 11 May 2021

Published online 2 August 2021 in Wiley Online Library (wileyonlinelibrary.com). DOI: 10.1002/mds.28671

In Parkinson's disease (PD), a progressive degeneration of the dopaminergic neurons located in the substantia nigra pars compacta (SNpc) results in an impaired control of voluntary movements and motor learning disturbances.<sup>1</sup> Early motor symptoms of most PD forms are evident when a 60%–70% loss of dopaminergic neurons causes a marked decrease in the striatal dopamine (DA) levels.<sup>2</sup>

Although significant advances in the last decade made it possible to recognize earlier signs of the disease, current treatments, mainly aimed at replacing DA levels in target areas, are unable to arrest neuronal degeneration or limit the side effects of current therapies. An intriguing but unexplored possibility is the combined use of innovative diagnostic markers into synergistic approaches that would preserve and enhance patients' brain residual functions, to maximize the responses to neurorehabilitation and pharmacotherapy treatments. Repetitive transcranial magnetic stimulation (rTMS), a noninvasive therapeutic approach to study neural network organization, used for diagnostic and therapeutic purposes, is an excellent candidate to meet these criteria. A single session (acute) treatment produces an increase in DA content in subcortical nuclei and induces temporary plasticity in target areas, effects that can be studied in human subjects and laboratory animals.<sup>3–6</sup>

The neurotoxin-based models of PD, the first experimental paradigms to provide significant insights into disease mechanisms, have the considerable advantage to induce a clear phenotype and a modular induction of neurodegeneration, providing a translational vision over the pathological and phenotypic characteristics of the human disease.<sup>7</sup> Among these, a proper use of 6-hydroxydopamine (6-OHDA) lesion model leads to distinct degrees of nigrostriatal denervation<sup>8,9</sup> and provides a glimpse of the neuronal alterations likely associated with the motor disturbances observed in PD patients. In 6-OHDA-partially-denervated rats (partial), showing mild motor alterations, a 70% reduction in striatal DA levels is sufficient to selectively impair the induction of corticostriatal long-term potentiation (LTP), which depends on N-methyl-D-aspartate receptors (NMDAR) activation, but not the induction of the long-term depression (LTD).<sup>9</sup>

A number of preclinical studies have provided evidence that rTMS induces changes in glutamatergic and dopaminergic systems,<sup>10,11</sup> suggesting that it may have an impact on excitatory synapses modulated by DA neurotransmission. However, no studies have so far explored the mechanisms underlying *ex vivo* long-term effects of rTMS at the early stages of PD.

Here, we explored potential beneficial effects of rTMS, using an intermittent theta-burst stimulation (iTBS) pattern in an experimental condition in which striatal DA levels are lowered to the threshold

associated with early motor symptoms in newly diagnosed PD patients.

To this aim, we used a partial 6-OHDA lesion to mimic the levels of DA cell loss in the early stages of PD. In this condition, reduced corticostriatal LTP is associated with an altered balance between GluN2A- and GluN2B-NMDAR subunits.<sup>9</sup> In line with a previous study showing that, among neuronal populations, immediate early gene activation is restricted to spiny projection neurons (SPNs),<sup>10</sup> we assumed that striatal neurons could be responsive to iTBS and proposed to analyze changes in dendritic spine density and morphometric measurements, and corticostriatal plasticity as a neuronal correlate of forelimb movement control.

Based on these premises, we tested the hypothesis that iTBS may reduce forelimb akinesia, a form of motor disability that consists of a dysfunctional control of voluntary movements in the front paw contralateral to the brain lesion side, efficiently measured with the stepping test and associated with striatal alterations in unilaterally lesioned animals.<sup>9,10,12</sup> We, also, hypothesized that iTBS could rescue corticostriatal LTP through an NMDAR-dependent mechanism. By using behavioral, immunohistochemical, and electrophysiological analyses, we explored structural and functional changes in SPNs of 6-OHDA-partially-lesioned rats that were exposed to acute iTBS *in vivo* 20 minutes before tissues and slices preparation.

## Materials and Methods

Extended methods can be found in the Appendix S1.

### Nigrostriatal Lesion

Male Wistar rats ( $n = 115$ , 1-month-old, 100–125 g at the time of the lesion) were deeply anesthetized and unilaterally injected with either saline (sham-operated, sham  $n = 39$ ) or 6-OHDA hydrochloride (Sigma Aldrich, Milan, Italy) dissolved in a 0.1% ascorbic acid solution in saline ( $n = 76$ ) into the medial forebrain bundle (MFB) of the left hemisphere (anteroposterior [AP] =  $-4.4$ , mediolateral [ML] =  $+1.2$  from Bregma, dorsoventral [DV] =  $-7.8$  from dura mater) as previously reported.<sup>13</sup>

Fifteen days later, 6-OHDA-lesioned rats were challenged for apomorphine-induced contralateral turning behavior to evaluate their DA-depleted status and be selected as partially ( $n = 62$  rats, indicated in the text as “partial”) and fully denervated ( $n = 14$  rats, indicated as “full”).<sup>9</sup> Rats that performed 0–10 turns were deemed to be unlesioned ( $n = 16$ ) and were excluded from this study. All the behavioral, morphological, and

electrophysiological experiments were performed 2 months after the lesion (Fig. 1A).

### Theta-Burst Stimulation

Sham-operated and 6-OHDA-lesioned rats were subjected to a single placebo or iTBS session. The iTBS protocol consisted in 10 trains of 50 Hz bursts (3 pulses), repeated at 5 Hz, applied every 10 s (300 pulses, 2 minutes total duration), using a DuoMAG XT-100 stimulator through a 70BF butterfly coil (DEYMED Diagnostic Europe, Czech Republic).<sup>10</sup> Based on the manufacturer's information and on previous studies using a similar experimental setting,<sup>14</sup> we considered that at a distance of 1 cm from the coil, an inducing current of 30% of maximal output produces a magnetic field strength of 0.5 T. This stimulation protocol, taking into account the dimensions of the rat's skull, induces a weak electric field as estimated by Funke et al.<sup>14</sup>

### Behavioral Testing of Motor Deficits, Stepping Test

The stepping test was used as previously reported.<sup>9</sup> Partial rats were tested, and their motor dysfunctions assessed before being randomly allotted into two groups receiving either placebo or iTBS stimulation.

### Electrophysiology

Animals were sacrificed 20 minutes post-stimulation. Corticostriatal coronal slices were obtained, and glutamatergic excitatory postsynaptic potentials (EPSPs) were evoked in intracellular and whole-cell patch-clamp recordings as previously described.<sup>13,15</sup> LTP and LTD were induced through a high-frequency stimulation (HFS) protocol in magnesium-free and physiological medium, respectively.<sup>16,17</sup> For studying spontaneous excitatory postsynaptic currents (sEPSCs), picrotoxin (50  $\mu$ M) was added to block GABA<sub>A</sub>-mediated currents.

### Dendritic Spine Analysis on Golgi-Stained Brains

Brains of full and partial animals were dissected, and the two hemispheres were impregnated separately in a Golgi-Cox solution (1% potassium dichromate, 1% mercuric chloride, 0.8% potassium chromate) at room temperature (RT). Samples were then placed in sucrose 30% for 3 days, sectioned, and mounted.<sup>18</sup> Dorsolateral SPNs were identified under low magnification (20  $\times$  0.5 numerical aperture [NA]) using an optical microscope DMLB Leica (Leica Microsystems, Milano, Italy). Dendritic spines were quantified online at a magnification of 100  $\times$  1.5 NA using a camera connected to the microscope. Spine density was measured on dendrites of fully impregnated dorsolateral SPNs ( $n = 4/5$

neurons per animal, 4/5 segments per neuron) by means of the Neurolucida software. Number of spines counted on dendrite segments of the same neuron were pooled together to obtain averaged values. Analysis of dendritic spines size was carried out on random selection of dendritic spines by measuring spine width parallel to dendrite through the ImageJ software (National Institutes of Health) (600 spines per group). Spine diameter values were expressed as cumulative frequencies.

### Dendritic Spine Analysis on Biocytin-Filled Neurons

After the recording, slices containing biocytin-loaded cells were fixed with 4% paraformaldehyde in 0.1 M phosphate-buffered saline (PBS) overnight at 4°C. The day after, the slices were washed in PBS and incubated with 555-conjugated Streptavidin (1:200; Streptavidin, Alexa Fluor 555 conjugate) in PBS 1% Triton X-100 for 3 hours at RT. Images were acquired using a Zeiss CLSM700 confocal laser-scanning microscope (Zeiss, Oberkochen, Germany). Neurons of interest were identified on a 10 $\times$  objective, and spines were captured with a 63 $\times$  oil immersion, objective zoom factor 1.0. After images acquisition, dendritic segments were analyzed for spine density, spine area, spine diameter, and spine neck diameter using the Imaris 7.6.5 software (Bitplane AG, Zürich, Switzerland).

### Tyrosine Hydroxylase Immunofluorescence Labeling and Analysis

Coronal sections were collected in PBS and incubated with mouse monoclonal anti-Tyrosine Hydroxylase (TH) antibody (1:300, Millipore, Milano, Italy) overnight at 4°C. Subsequently, they were incubated with secondary antibody Alexa Fluor 594 goat anti-rabbit for 2 hours at RT, avoiding light. DAPI staining (1:1000, Enzo Life Science, Milano, Italy) was performed at the last wash with PBS. Images of TH staining in Substantia Nigra (SN) were acquired using Zeiss CLSM700 confocal laser-scanning microscope (Zeiss) and captured with a 5 $\times$  objective. To evaluate the number of dopaminergic neurons, TH-positive cells from both hemispheres were counted in 3–5 slices cut at  $-4.68$  to  $-6.00$  mm from Bregma.

### Statistical Analysis

Analyses were performed using Prism 6.0 (GraphPad Software, San Diego, CA, USA). Paired and unpaired Student's *t* tests were used for the behavioral analysis to evaluate motor dysfunctions. Paired Student's *t* test was used to compare values of the EPSPs amplitudes of the pre- versus (vs.) post-HFS protocol in the same cell population. Statistical comparisons of the EPSPs mean amplitude were analyzed over time between different neuronal

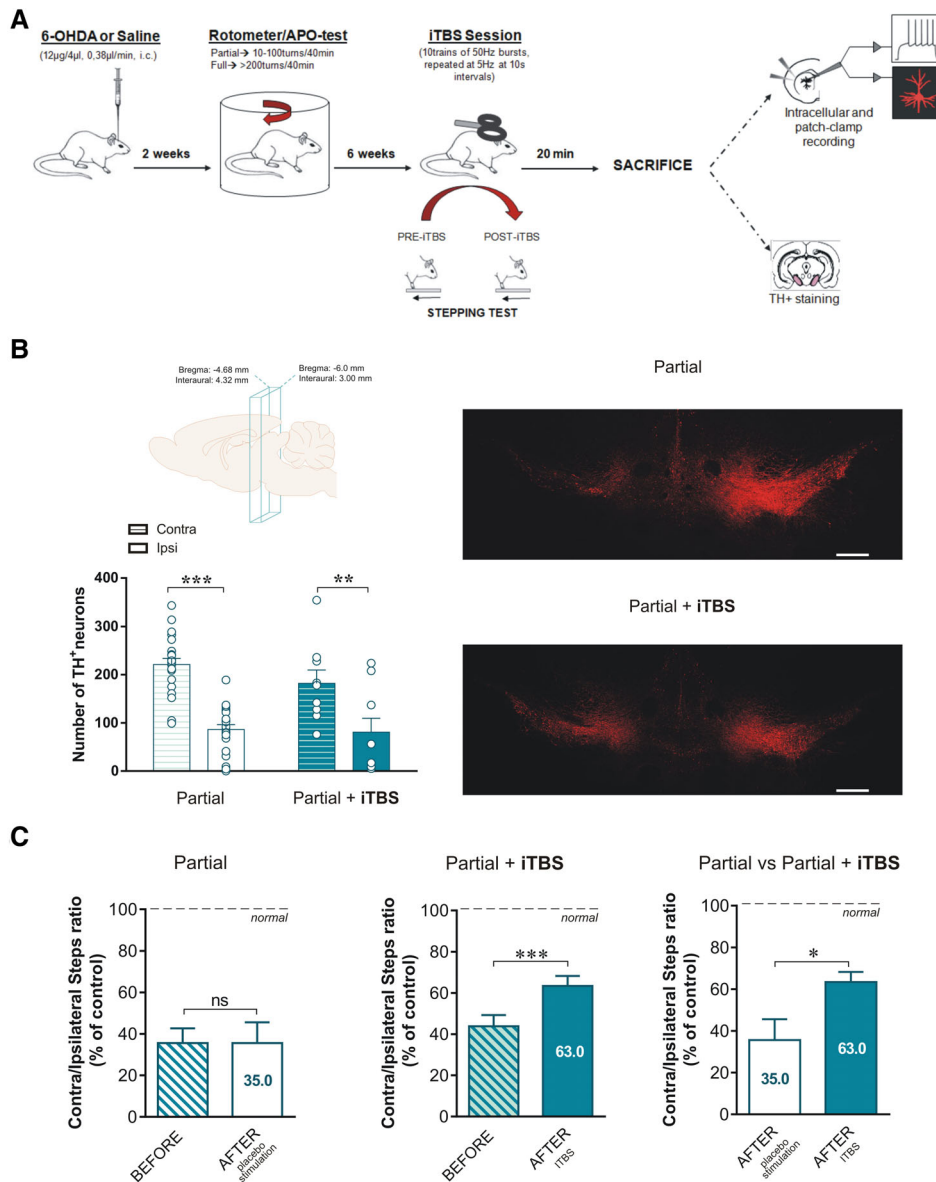


**FIG. 1.** Experimental plan and model assessment. **(A)** Time plan of experimental procedures. **(B)** Left, upper panel: schematic representation of the rat brain with the stereotaxic coordinates of the coronal midbrain sections used for immunohistochemical analysis. Lower panel: number of TH-positive neurons in the two hemispheres ipsilateral (ipsi) and contralateral to the lesion side (contra), in the midbrain of animals with Partial lesion subjected to placebo stimulation (Partial) or iTBS (Partial+iTBS). Right: images of coronal midbrain sections from Partial rats subjected to placebo stimulation or iTBS. Scale bar, 500 µm. Data are plotted as mean ± SEM. **(C)** Histograms show the averaged ratio, expressed as a percentage of control, between the number of contralateral and ipsilateral steps made by Partial rats with their forelimbs during each trial before and after being exposed to placebo stimulation (Partial) or with iTBS (Partial+iTBS). Data are reported as mean ± SEM.

populations using a two-way ANOVA. Current–voltage (I–V) curves were compared using one-way ANOVA. Morphological (Golgi-based spine scores) measurements were compared by means of two-way ANOVA with site of the lesion (ipsilateral lesioned vs. contralateral non-lesioned hemisphere) and treatment (iTBS vs. placebo stimulation) as main factors. A two-way ANOVA was performed after assessment of the distribution normality by means of the Shapiro–Wilk test. If the interactions were significant, the test was followed by Bonferroni’s for

post hoc comparison. Spine density scores obtained from biocytin-filled partial and partial+iTBS neurons were compared by means of a Mann–Whitney *U* test as one sample distribution did not conform with the normality test. Cumulative frequencies of spine head diameters in partial vs. partial+iTBS and full vs. full+iTBS were compared by means of the Kolmogorov–Smirnov (KS) test. Values given in the text and the figures are mean ± SEM of changes in the respective cell populations. An  $\alpha$  level of 0.05 was used for all statistical tests.

## Results

### Nigrostriatal Lesion Extents Are Indistinguishable in the Experimental and Sham Cohorts

Quantification of dopaminergic cells in the SNpc of partial rats exposed to iTBS ( $n = 4$  rats) or placebo stimulation ( $n = 5$  rats) (Fig. 1A) was carried out by counting TH-positive cells in the left hemisphere where the unilateral stereotaxic injections of the neurotoxin 6-OHDA were performed (ipsilateral) and comparing these values to those of the non-lesioned right hemisphere (contralateral).<sup>9,19,20</sup> Statistical comparisons by two-way ANOVA confirmed a significant effect of the lesion ( $F_{(1,62)} = 45.51$ ,  $P < 0.001$ ) but no effect of the iTBS treatment ( $F_{(1,62)} = 1.460$ ,  $P = 0.23$ ) and no significant lesion  $\times$  treatment interaction ( $F_{(1,62)} = 0.786$ ,  $P = 0.37$ ). A 70% reduction of the number of TH-positive cells was found in the left hemisphere of partial rats regardless of the treatment (Fig. 1B,  $P < 0.01$  for each pair comparison).

### Acute iTBS Improves Forelimb Akinesia and Limb Use Asymmetry in Partial Rats

The effect of iTBS on motor dysfunctions in partial rats ( $n = 16$  rats) was evaluated by means of the stepping test, which estimates forelimb akinesia and limb-use asymmetry via the calculation of the contralateral/ipsilateral step ratio.<sup>9</sup> Partial rats showed an improvement in the use of the contralateral (impaired) forelimb after exposure to iTBS, compared to their pre-stimulation state (Fig. 1C, central panel; paired Student's  $t$  test before vs. after iTBS treatment,  $t = 5.061$ ,  $df = 8$ ,  $***P < 0.001$ ). Post-stimulation comparison of contralateral/ipsilateral steps ratios revealed that partial rats exposed to iTBS used significantly more the contralateral impaired forelimb than their counterparts receiving the placebo stimulation (Fig. 1C, right panel; unpaired Student's  $t$  test, after iTBS vs. placebo stimulation,  $t = 2703$ ,  $df = 14$ ,  $*P < 0.05$ ).

### Intrinsic Membrane Properties and LTD of SPNs in Sham and Partial Rats Are Unchanged by iTBS

Intrinsic membrane properties of SPNs were examined in each condition by performing intracellular and whole-cell patch-clamp recordings (Fig. S1A). The current-voltage curve (I-V), representing the responses of the membrane to current steps of increasing intensity before crossing the firing threshold, was unaltered after exposure to iTBS in any condition (upper-right panel). Two-way ANOVA analysis was used to compare the changes in the membrane potential in response to increasing stimulation (time effect  $F_{(5,135)} = 349.15$ ,  $P < 0.0001$ , treatment effect  $F_{(3,27)} = 1.914$ ,  $P = 0.15$ ,

ns, and time  $\times$  treatment interaction,  $F_{(15,135)} = 1.344$ ,  $P = 0.19$ , ns). The mean number of spikes, calculated at the step of 500 pA, was also similar among groups (representative traces on the left panel and whisker plot graph on the lower-right panel) (Sham:  $19.40 \pm 1.50$  ( $n = 6$ ), Sham+iTBS:  $19.75 \pm 2.10$  ( $n = 5$ ), Partial:  $20.50 \pm 1.85$  ( $n = 6$ ) and Partial+iTBS:  $18.75 \pm 1.25$  ( $n = 5$ ); one-way ANOVA:  $F_{(3,13)} = 0.1763$ ,  $P = 0.91$ , ns). The resting membrane potential (RMP) values, calculated at 0 pA from the I-V curve, were also in the same range in all experimental conditions (Fig. S1A, average values:  $-90.13 \pm 1.98$  mV for Sham rats ( $n = 9$ );  $-89.84 \pm 1.70$  mV for Sham+iTBS rats ( $n = 10$ );  $-86.60 \pm 1.65$  mV for Partial ( $n = 8$ );  $-86.43 \pm 1.45$  mV for Partial+iTBS ( $n = 8$ )).

The effect of iTBS on long-term synaptic plasticity was evaluated using a HFS protocol shown to elicit LTD at corticostriatal synapses in conditions where the activation of  $\alpha$ -amino-3-hydroxy-5-methyl-4-isoxazolepropionic acid (AMPA) receptor is prevalent, and both DA D1 and D2 receptors are activated.<sup>16,21</sup> Results show a regular induction and maintenance of LTD regardless of the treatment, both in sham (Fig. S1B; paired Student's  $t$  test, pre- vs. 30 minutes post-HFS, Sham:  $t = 7.496$ ,  $df = 11$ ,  $P < 0.001$ ,  $n = 6$ ; Sham+iTBS,  $t = 6.421$ ,  $df = 21$ ,  $***P < 0.001$ ,  $n = 11$ ) and in partial rats (Fig. S1B; paired Student's  $t$  test, pre- vs. 30 minutes post-HFS, Partial:  $t = 14.16$ ,  $df = 13$ ,  $***P < 0.001$ ,  $n = 7$ ; Partial+iTBS:  $t = 7.178$ ,  $df = 11$ ,  $***P < 0.001$ ,  $n = 6$ ). These observations were confirmed by a two-way ANOVA analysis showing no significant group  $\times$  time interaction in both sham ( $F_{(18,270)} = 0.2615$ ,  $P = 0.99$ , ns) and partial rats ( $F_{(18,198)} = 0.7619$ ,  $P = 0.74$ , ns).

### A Single Session of iTBS Induces Synaptic and Plastic Changes in Partial Rats

Spontaneous glutamatergic synaptic activity was recorded in slices using the whole-cell patch-clamp technique. Partial rats that had undergone a placebo stimulation, exhibited an increase in the amplitude, but not the frequency, of sEPSCs compared to sham rats (Fig. 2A, one-way ANOVA, amplitude:  $F_{(3,36)} = 10.72$ ,  $P < 0.01$ ,  $n = 13$  Sham vs.  $n = 9$  Partial; frequency:  $F_{(3,33)} = 0.7255$ ,  $P = 0.54$ , ns). The exposure to iTBS fully rescued both the increase in sEPSCs amplitude in partial rats ( $n = 9$  Partial vs.  $n = 7$  Partial+iTBS,  $P < 0.05$ ) and the concurrent increase in sEPSCs amplitude and frequency previously reported<sup>13,21</sup> in fully-lesioned (Full) rats (Fig. S3A, unpaired Student's  $t$  test, frequency:  $n = 12$  Full vs.  $n = 10$  Full+iTBS,  $t = 5.160$ ,  $df = 19$ ,  $***P < 0.001$  and amplitude:  $n = 9$  Full vs.  $n = 11$  Full+iTBS,  $t = 3.852$ ,  $df = 18$ ,  $**P < 0.01$ ). The propensity of SPNs to express a persistent corticostriatal LTP was studied in partial and sham rats in each stimulation

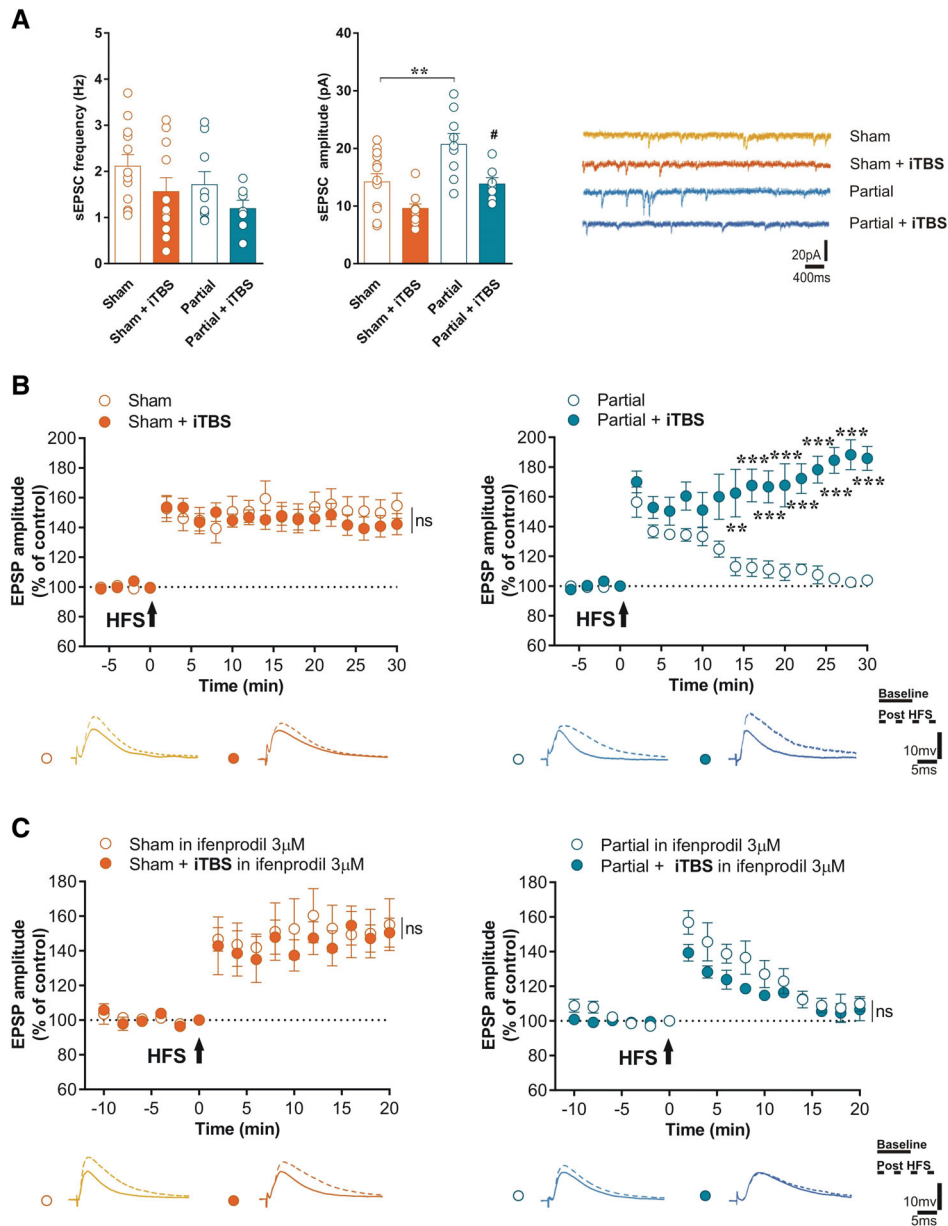


**FIG. 2.** Synaptic and plastic changes induced by a single session of iTBS in partially lesioned rats. **(A)** Frequency and amplitude of sEPSC recorded from SPNs of Sham and Partial rats 20 minutes after placebo stimulation (Sham, Partial) or iTBS (Sham+iTBS, Partial+iTBS). Representative traces (right panel) show sEPSCs events in SPNs of the four different experimental groups. Data are plotted as mean  $\pm$  SEM. **(B)** Time course (upper panel) of mean EPSP amplitude of SPNs in response to an LTP protocol applied in corticostriatal slices from Sham and Partial animals 20 minutes after a session of placebo stimulation (Sham and Partial) or iTBS (Sham+iTBS and Partial+iTBS). Representative traces (lower panels) of single SPN recorded from Sham, and Sham+iTBS or Partial and Partial+iTBS, before (solid lines) and after HFS (dotted lines). **(C)** Time course (upper panel) of mean EPSP amplitude in SPNs recorded from Sham, Sham+iTBS, Partial and Partial+iTBS after induction of LTP protocol in the presence of 3  $\mu$ M ifenprodil. Representative traces (lower panels) of single SPNs recorded from the four experimental groups.

condition. Consistent with previous observations,<sup>10,17</sup> HFS applied in sham rats elicited a NMDA- and D1-receptor-dependent LTP of corticostriatal transmission that was unaffected by iTBS (Fig. 2B, paired Student's *t* test, Sham pre- vs. 30 minutes post-HFS,  $t = 10.04$ ,  $df = 9$ ,  $***P < 0.001$ ,  $n = 7$ ; Sham+iTBS pre- vs. 30 minutes post-HFS,  $t = 8355$ ,  $df = 11$ ,  $***P < 0.001$ ,  $n = 9$ ). As expected,<sup>9</sup> HFS applied to placebo-stimulated partials did not elicit a lasting LTP

(Partial pre- vs. 30 minutes post-HFS,  $t = 2032$ ,  $df = 9$ ,  $P > 0.5$ ,  $n = 5$ ) but instead a short-term potentiation of EPSP amplitude that returned to baseline values in 15 minutes. Application of iTBS was associated to an efficient maintenance of LTP that persisted over the recording time in the partial SPNs (Partial+iTBS pre- vs. 30 minutes post-HFS,  $t = 13,98$ ,  $df = 11$ ,  $***P < 0.001$ ,  $n = 6$ ; two-way ANOVA, time  $\times$  group interaction,  $F_{(14,126)} = 10.37$ ,  $P < 0.001$ ;  $P < 0.01$  at 14 minutes and

$P < 0.001$  from 16–30 minutes post-HFS). To explore the nature of this iTBS-induced LTP, we based our approach on the consideration that in healthy rats, GluN2A- but not GluN2B-expressing NMDARs are selectively required for the induction of LTP, which largely relies on the observation that application of selective non-competitive antagonist of the GluN2B subunit, ifenprodil, leaves corticostriatal LTP unaltered.<sup>22</sup> Because partial rats show an increase in GluN2A/2B ratio receptor subunit composition,<sup>9</sup> we tested the hypothesis that iTBS could rebalance GluN2A/2B ratio by increasing GluN2B-mediated activity. To contrast this effect of iTBS, we first applied ifenprodil in slices from sham rats placebo stimulation where, as expected, it did not affect LTP (Fig. 2C, Paired Student's  $t$  test, Sham pre- vs. 30 minutes post-HFS,  $t = 5.440$ ,  $df = 11$ ,  $***P < 0.001$ ,  $n = 6$ ). We, then, applied the HFS protocol to induce LTP in slices of partials that received placebo or iTBS, and recorded changes in EPSP amplitude under ifenprodil application for the entire duration of the recording. The application of the GluN2B antagonist in corticostriatal slices from partial+iTBS rats before the HFS completely blocked the induction of the otherwise observed iTBS-associated LTP (Fig. 2C, Partial+iTBS pre- vs. 30 minutes post-HFS,  $t = 1.516$ ,  $df = 15$ ,  $P > 0.5$ ,  $n = 6$ ).

### iTBS Increases Total Spine Density and the Proportion of Thin Spines on SPNs of Partial Rats

Given that signaling through NMDARs is required to induce structural plasticity in dendritic spines,<sup>23,24</sup> we performed unbiased measurements of dendritic spine density in Golgi-stained SPNs in the lesioned (ipsilateral) and the non-lesioned (contralateral) hemisphere of partials exposed to iTBS or placebo stimulation (Fig. 3A). A two-way ANOVA revealed an effect of the site of lesion ( $F_{(1,47)} = 12.02$ ,  $P < 0.01$ ), of treatment ( $F_{(1,47)} = 20.67$ ,  $P < 0.01$ ), and a significant site of the lesion  $\times$  treatment interaction ( $F_{(1,47)} = 14.60$ ,  $P < 0.01$ ). Post hoc pair comparisons then showed that fewer spines were counted on SPNs in the ipsilateral hemisphere than in the contralateral hemisphere ( $P < 0.001$ ), which confirms the disruptive effect of the 6-OHDA lesion on synaptic density.<sup>25</sup> Notably, iTBS increased spine density in SPNs in the lesioned hemisphere (Partial vs. Partial+iTBS,  $P < 0.001$ ) and rescued inter-hemispheric differences in spines (Partial+iTBS ipsilateral vs. contralateral ( $P = 0.79$ , ns) (Fig. 3B,C). Full+iTBS rats also showed an increase in spines in the ipsilateral hemisphere (Full vs. Full+iTBS,  $P < 0.001$ ), which, however, did not fully rescue the inter-hemispheric differences in spines (Full+iTBS ipsilateral vs. contralateral,  $P < 0.05$ , Fig. S3B). Aside from the net number of spines, which globally depicts synaptic

density, morphological parameters as the size and shape of spines are indexes of the maturation and stability of synapses, with the large spines hosting robust synapses.<sup>26</sup>

Accordingly, we measured spine head diameters on neurons in the ipsilateral hemisphere from partial and partial+iTBS rats. Cumulative frequency graphs showed a shift to the left of the partial+iTBS curve, which reveals that the stimulation significantly increased the proportion of thin spines in the lesioned rats (Fig. 3D, KS,  $D = 0.3$ ,  $P < 0.001$ ). To establish direct correlations between electrophysiological and morphological changes, spine density and spine head diameters were also measured in a smaller sample of previously recorded biocytin-filled neurons from Partial and Partial+iTBS rats (Fig. 3E,F). Consistent with the Golgi data, iTBS increased both spine density (Fig. 3G; Partial vs. Partial+iTBS,  $U = 5$ ,  $*P < 0.05$ ) and the proportion of thin spines (Fig. 3H, mean diameter KS,  $D = 0.4002$   $P < 0.001$ ) in the ipsilateral hemisphere. Additional measurements automatically detected by Imaris software in biocytin-filled neurons showed that spines in partial+iTBS also had smaller head areas (Fig. S2A,  $U = 0.0$ ,  $***P < 0.01$ ) and neck diameters (Fig. S2B mean diameter  $D = 0.4002$   $P < 0.001$ ), consistently with their immature status.

Overall, the morphological data demonstrate that iTBS applied to the lesioned dorsolateral striatum triggers an increase in the density of thin, immature, and potentially more plastic dendritic spines, which are typically observed in developing neurons. These newly formed spines are likely to be seen as a key structural component involved in the recovery of synaptic plasticity observed following the same treatment (Fig. 3I).

## Discussion

In the paradigm used here, modeling early symptomatic PD, a partial loss of dopaminergic afferents onto striatal SPNs, results in the manifestation of mild akinesia, a potentiation of spontaneous synaptic currents and a deficit in activity-dependent LTP. These alterations in behavior and plasticity were previously associated with a GluN2A/GluN2B unbalance, considered at the origin of motor, behavioral, and synaptic plasticity defects.<sup>9</sup> Here, by demonstrating that application of iTBS in early parkinsonian rats alleviated motor dysfunctions, fully rescued corticostriatal LTP, and triggered the induction of immature dendritic spines in SPNs, we provide evidence that acute iTBS rescues the phenotype and identify a novel mechanism of compensatory adaptation in the parkinsonian basal ganglia circuitry, which supports the observed recovery.

In full experimental parkinsonism, a characteristic increase in both frequency and amplitude of spontaneous

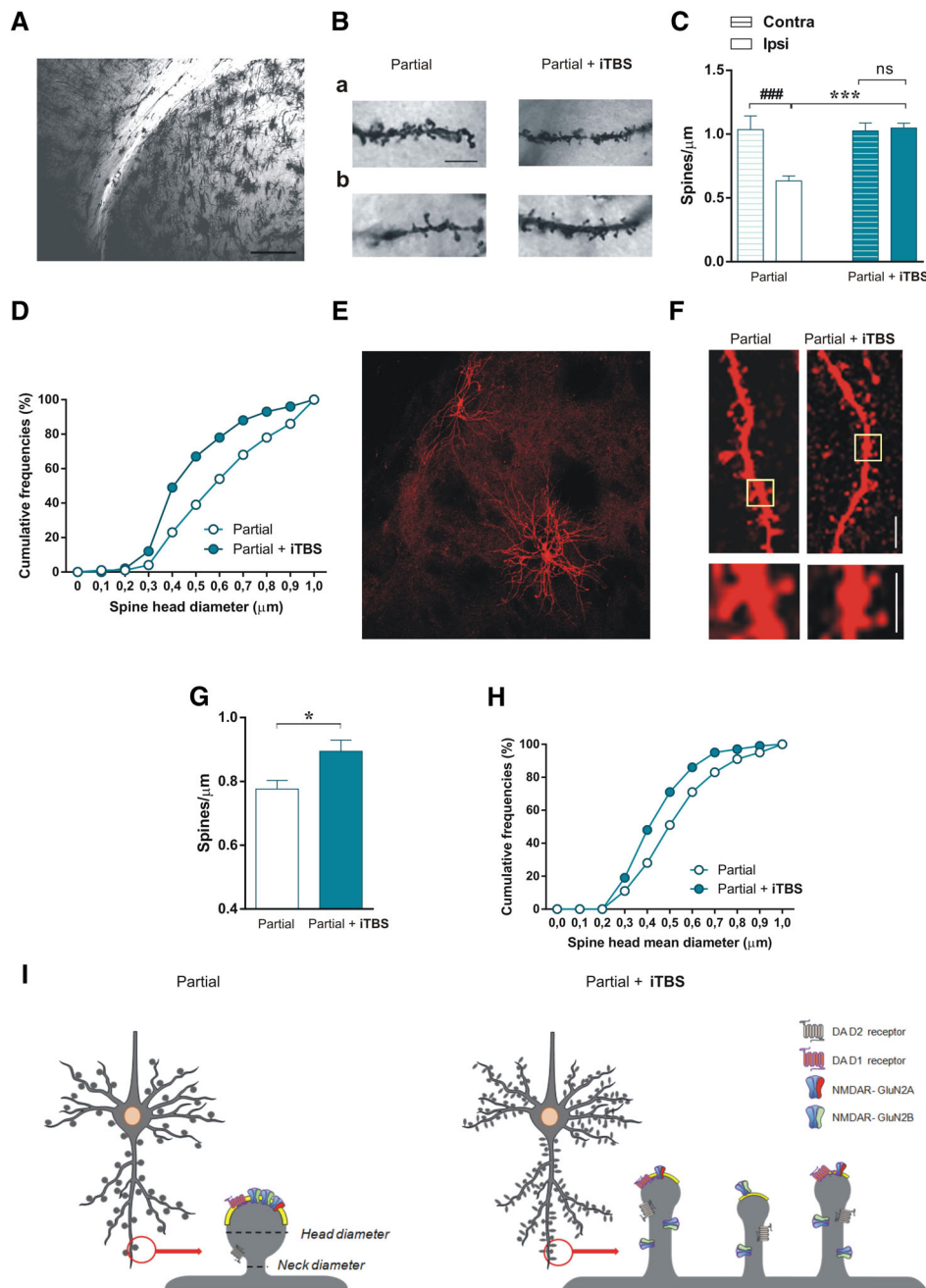


**FIG. 3.** Acute iTBS increases total spine density and the proportion of thin spines on SPNs of Partial rats. **(A)** Representative images of Golgi staining in the neurons of dorsolateral striatum acquired at  $5\times$  magnification (scale bar,  $250\ \mu\text{m}$ ). **(B)** Photomicrographs of Golgi-stained neurons showing dendritic segments from contralateral (a) and ipsilateral (b) hemisphere of Partial and Partial+iTBS rats (scale bar,  $10\ \mu\text{m}$ ). **(C)** Spine density values in Golgi-stained dendrites of Partial and Partial+iTBS rats. Data are plotted as mean  $\pm$  SEM; (3 hemisphere/group, 3–5 neurons/hemisphere). **(D)** Cumulative frequencies of spine head diameter measured on Golgi stained samples. **(E)** Image of a biocytin-loaded neuron recorded from rat coronal slice ( $5\times$  magnification, scale bar,  $50\ \mu\text{m}$ ). **(F)** Biocytin-filled dendritic segment from Partial and Partial+iTBS rats (scale bar,  $5\ \mu\text{m}$ ). Yellow squares in the upper panels refer to areas magnified in the bottom panels (scale bar,  $2.5\ \mu\text{m}$ ). **(G)** Spine density values (n spines/ $\mu\text{m}$ ) **(H)** Cumulative frequencies of spine head mean diameter obtained from biocytin-filled dendrites of Partial and Partial+iTBS rats. **(I)** Schematic representation of the morphological changes observed in the dorsolateral SPNs of partial rats that received placebo (left panel) or iTBS stimulation (right panel).

glutamatergic activity because of a disrupted DA-glutamate interplay is observed.<sup>21</sup> Here, we show for the first time that an incomplete nigrostriatal lesion, aside from being associated with mild motor symptoms and with a selective alteration of LTP, is also linked to a

specific alteration of the spontaneous glutamatergic activity limited to its amplitude. Such an increase in amplitude was rescued by iTBS, according to our hypothesis that a complete recovery can be observed when the iTBS is delivered in rats with a consistent pool of preserved TH-



positive neurons. The further observation that iTBS rescues the increase in amplitude and frequency of EPSCs in fully parkinsonian rats<sup>13,21</sup> unveils an unexpected efficacy of the stimulation on excessive glutamatergic activity.

Concerning the effects of magnetic stimulation on synaptic plasticity in partial rats, whereas LTD remained unaltered following iTBS application, the LTP deficit was rescued, suggesting that the stimulation interferes explicitly with the damaged synaptic operations without detrimental effects on preserved functions. This result agrees with a previous study showing a time-dependent area- and cell-type-specific c-Fos activation following iTBS treatment in parkinsonian rats.<sup>10</sup> Therefore, the spectrum of SPNs synaptic deficits normalized by iTBS complements the deficits observed at the different degrees of DA denervation.

Relevant to the possible mechanisms underlying the rescue of LTP, in a seminal study, Paillé and colleagues showed an unbalanced GluN2A/GluN2B subunit ratio in the striatal postsynaptic density of the partial rats as the mechanism preventing LTP expression.<sup>9</sup> Based on this assumption, we wondered whether the iTBS-induced recovery of LTP could be ascribed to a rearrangement of the NMDAR subunits ratio. In the adult striatum, GluN2A is required for LTP expression, and the GluN2B antagonist does not affect LTP induction.<sup>22</sup> In early PD, NMDAR subunits unbalance depends on the abnormal elevation of GluN2A in the dorsal striatum.<sup>9</sup> Instead of favoring LTP, such condition brings to a marked reduction of its maintenance, leading to the concept that more than the level of a specific subunit (each exhibiting strikingly unique biophysical and pharmacological properties), a balanced interaction between the two is rather required for LTP induction. Therefore, we hypothesized that iTBS could also change the ratio by either decreasing GluN2A or increasing GluN2B-mediated functions. The more sustainable and simple way to test this hypothesis was to contrast a possible increase of GluN2B by iTBS with a GluN2B antagonist. In line with these premises, in partial rats exposed to iTBS, ifenprodil was able to vanish the induction of this form of restorative plasticity. Interestingly, ifenprodil alone, without iTBS, did not further shorten the duration of typical short-term potentiation in partial rats exposed to placebo stimulation.

Such functional enhancement in GluN2B function, bringing to a plasticity recovery, raised the question as to whether iTBS could trigger some form of structural remodeling in SPNs. To answer this question, we measured the density and shape of dendritic spines, subcellular elements that host the majority of excitatory synapses in SPNs. Parallel analyses were carried out in Golgi-Cox impregnated and in a small sample of previously recorded biocytin-filled neurons. Confirming that dendritic spine loss is a robust feature of experimental and human parkinsonism,<sup>25,27-30</sup> our data show that

partial rats exhibited a decreased spine density on SPNs in the lesioned hemisphere that was fully rescued by iTBS stimulation. The recovery of spine density in the partial+iTBS group was associated with an increase in the proportion of thin spines, (ie, small spines with reduced head and neck diameters) typically observed in developing neurons.

Interestingly, thin spines of juvenile excitatory synapses require GluN2B-expressing NMDARs enrichment.<sup>31-33</sup> These receptors are thought to preserve the immature status of excitatory synapses during synaptogenesis, making both functional and structural changes easier to occur.<sup>34</sup> Considering that thin spines are the subcellular sites where responsive neurons build transient and flexible synapses, we speculate that iTBS triggers a juvenile-like remodeling that, if appropriately stimulated by HFS, drugs, genetic manipulations, or exploited in motor learning tasks, would maximize the effect of pharmacological and neurorehabilitation approaches. Although exploratory, our findings show that the formation of new spines after iTBS also occurs in biocytin-filled neurons. This consistency implies that the two methods validate each other and provides powerful information about the dimension of the phenomenon observed, reinforcing our assumption that iTBS significantly modifies these parameters also in the recorded cells. This fact confirms that the formation of new dendritic spines after iTBS is a key structural component underlying synaptic plasticity.

In conclusion, acute iTBS ameliorated motor symptoms and rescued functional and structural alterations specific to the early symptomatic stage of experimental PD. These effects involve a functional contribution of GluN2B-containing NMDARs, although the link of this involvement to possible increases of endogenous DA release associated with reduced inflammation, as previously observed in fully denervated animals,<sup>10</sup> has not been demonstrated yet. However, by identifying the implication of a specific receptor subunit, our data shed light on a novel mechanism by which iTBS exerts its actions and provide a molecular target to explore and promote new studies on the use of noninvasive stimulation as an efficient add-on to current therapies. ■

**Acknowledgments:** This work was supported by grants from the Fresco Parkinson Institute to New York University School of Medicine and The Marlene and Paolo Fresco Institute for Parkinson's and Movement Disorders, which were made possible with support from Marlene and Paolo Fresco (V.G., P.C., and A.C.) and by the Italian Ministry of Health, Ricerca Corrente (B.P. and P.C.).

## Data Availability Statement

The data that support the findings of this study are available from the corresponding author upon reasonable request.

## References

1. Fahn S. Description of Parkinson's Disease as a Clinical Syndrome. *Annals of the New York Academy of Sciences* 2006;991(1):1–14.
2. Bernheimer H, Birkmayer W, Hornykiewicz O, Jellinger K, Seitelberger F. Brain dopamine and the syndromes of Parkinson and Huntington. Clinical, morphological and neurochemical correlations. *J Neurol Sci* 1973;20(4):415–455.
3. Strafella AP, Paus T, Fraraccio M, Dagher A. Striatal dopamine release induced by repetitive transcranial magnetic stimulation of the human motor cortex. *Brain* 2003;126(Pt 12):2609–2615.
4. Funke K, Benali A. Modulation of cortical inhibition by rTMS - findings obtained from animal models. *J Physiol* 2011;589(Pt 18):4423–4435.
5. Huang YZ, Edwards MJ, Rounis E, Bhatia KP, Rothwell JC. Theta burst stimulation of the human motor cortex. *Neuron* 2005;45(2):201–206.
6. Soundara Rajan T, Ghilardi MFM, Wang HY, et al. Mechanism of action for rTMS: a working hypothesis based on animal studies. *Front Physiol* 2017;8:457.
7. Cenci MA, Ohlin KE. Rodent models of treatment-induced motor complications in Parkinson's disease. *Parkinsonism Relat Disord* 2009;15(Suppl 4):S13–S17.
8. Blandini F, Armentero MT, Martignoni E. The 6-hydroxydopamine model: news from the past. *Parkinsonism Relat Disord* 2008;14(Suppl 2):S124–S129.
9. Paille V, Picconi B, Bagetta V, et al. Distinct levels of dopamine denervation differentially alter striatal synaptic plasticity and NMDA receptor subunit composition. *J Neurosci* 2010;30(42):14182–14193.
10. Cacace F, Mineo D, Viscomi MT, et al. Intermittent theta-burst stimulation rescues dopamine-dependent corticostriatal synaptic plasticity and motor behavior in experimental parkinsonism: possible role of glial activity. *Mov Disord* 2017;32(7):1035–1046.
11. Moretti J, Poh EZ, Rodger J. rTMS-induced changes in glutamatergic and dopaminergic systems: relevance to cocaine and methamphetamine use disorders. *Front Neurosci* 2020;14:137.
12. Olsson M, Nikkhah G, Bentlage C, Bjorklund A. Forelimb akinesia in the rat Parkinson model: differential effects of dopamine agonists and nigral transplants as assessed by a new stepping test. *J Neurosci* 1995;15(5 Pt 2):3863–3875.
13. Bagetta V, Sgobio C, Pendolino V, et al. Rebalance of striatal NMDA/AMPA receptor ratio underlies the reduced emergence of dyskinesia during D2-like dopamine agonist treatment in experimental Parkinson's disease. *J Neurosci* 2012;32(49):17921–17931.
14. Benali A, Trippe J, Weiler E, et al. Theta-burst transcranial magnetic stimulation alters cortical inhibition. *J Neurosci* 2011;31(4):1193–1203.
15. Cerovic M, Bagetta V, Pendolino V, et al. Derangement of Ras-guanine nucleotide-releasing factor 1 (Ras-GRF1) and extracellular signal-regulated kinase (ERK) dependent striatal plasticity in L-DOPA-induced dyskinesia. *Biol Psychiatry* 2015;77(2):106–115.
16. Calabresi P, Maj R, Pisani A, Mercuri NB, Bernardi G. Long-term synaptic depression in the striatum: physiological and pharmacological characterization. *J Neurosci* 1992;12(11):4224–4233.
17. Calabresi P, Pisani A, Mercuri NB, Bernardi G. Long-term potentiation in the striatum is unmasked by removing the voltage-dependent magnesium block of NMDA receptor channels. *Eur J Neurosci* 1992;4(10):929–935.
18. Pignataro A, Borreca A, Ammassari-Teule M, Middei S. CREB regulates experience-dependent spine formation and enlargement in mouse barrel cortex. *Neural Plast* 2015;2015:651469.
19. Ghiglieri V, Mineo D, Vannelli A, et al. Modulation of serotonergic transmission by eltopazine in L-DOPA-induced dyskinesia: behavioral, molecular, and synaptic mechanisms. *Neurobiol Dis* 2016;86:140–153.
20. Picconi B, Centonze D, Hakansson K, et al. Loss of bidirectional striatal synaptic plasticity in L-DOPA-induced dyskinesia. *Nat Neurosci* 2003;6(5):501–506.
21. Calabresi P, Mercuri NB, Sancesario G, Bernardi G. Electrophysiology of dopamine-denervated striatal neurons. Implications for Parkinson's disease. *Brain* 1993;116(Pt 2):433–452.
22. Li P, Li YH, Han TZ. NR2A-containing NMDA receptors are required for LTP induction in rat dorsolateral striatum in vitro. *Brain Res* 2009;1274:40–46.
23. Hamilton AM, Oh WC, Vega-Ramirez H, et al. Activity-dependent growth of new dendritic spines is regulated by the proteasome. *Neuron* 2012;74(6):1023–1030.
24. Kwon HB, Sabatini BL. Glutamate induces de novo growth of functional spines in developing cortex. *Nature* 2011;474(7349):100–104.
25. Solis O, Limon DI, Flores-Hernandez J, Flores G. Alterations in dendritic morphology of the prefrontal cortical and striatum neurons in the unilateral 6-OHDA-rat model of Parkinson's disease. *Synapse* 2007;61(6):450–458.
26. Kasai H, Matsuzaki M, Noguchi J, Yasumatsu N, Nakahara H. Structure-stability-function relationships of dendritic spines. *Trends Neurosci* 2003;26(7):360–368.
27. Bellucci A, Mercuri NB, Venneri A, et al. Review: Parkinson's disease: from synaptic loss to connectome dysfunction. *Neuropathol Appl Neurobiol* 2016;42(1):77–94.
28. Gagnon D, Petryszyn S, Sanchez MG, et al. Striatal neurons expressing D1 and D2 receptors are morphologically distinct and differently affected by dopamine denervation in mice. *Sci Rep* 2017;7:41432.
29. Ingham CA, Hood SH, Arbuthnott GW. Spine density on neostriatal neurones changes with 6-hydroxydopamine lesions and with age. *Brain Res* 1989;503(2):334–338.
30. Matuskey D, Tinaz S, Wilcox KC, et al. Synaptic changes in Parkinson disease assessed with in vivo imaging. *Ann Neurol* 2020;87(3):329–338.
31. Barria A, Malinow R. Subunit-specific NMDA receptor trafficking to synapses. *Neuron* 2002;35(2):345–353.
32. Dong Y, Nestler EJ. The neural rejuvenation hypothesis of cocaine addiction. *Trends Pharmacol Sci* 2014;35(8):374–383.
33. van Zundert B, Yoshii A, Constantine-Paton M. Receptor compartmentalization and trafficking at glutamate synapses: a developmental proposal. *Trends in Neurosciences* 2004;27(7):428–437.
34. Gambrill AC, Barria A. NMDA receptor subunit composition controls synaptogenesis and synapse stabilization. *Proc Natl Acad Sci U S A* 2011;108(14):5855–5860.

## Supporting Data

Additional Supporting Information may be found in the online version of this article at the publisher's web-site.